Laboratory Investigation (2021) 101:897–907
https://doi.org/10.1038/s41374-021-00580-y

ARTICLE

Tubeimoside I improves endothelial function in sepsis via activation of SIRT3

Xiyang Yang[1,2] · Xingbing Li[1,2] · Minghao Luo[1,2] · Chang Li[1,2] · Longxiang Huang[1,2] · Xiang Li[1] · Bi Huang[1] · Jian Shen[1,2] · Suxin Luo[1,2] · Jianghong Yan[2]

Received: 20 November 2020 / Revised: 6 February 2021 / Accepted: 9 February 2021 / Published online: 4 March 2021

Abstract

Sepsis is life-threatening organ dysfunction caused by a deregulated host response to infection. Endothelial dysfunction is the initial factor leading to organ dysfunction and it is associated with increased mortality. There is no effective drug to treat sepsis-induced endothelial dysfunction. In this study, we detected a favorable effect of tubeimoside I (TBM) in ameliorating sepsis-induced endothelial dysfunction. To unveil the mechanism how TBM protects against sepsis-induced endothelial dysfunction, we examined TBM's effects on oxidative stress and apoptosis both in vivo and in vitro. TBM treatment alleviated oxidative stress by decreasing NOX2 and Ac-SOD2/SOD2 and decreased apoptosis by inhibiting cleaved caspse3 and Bax/Bcl-2. Notably, sepsis induced a significant decrease of SIRT3 expression in vascular endothelium, while TBM treatment reversed SIRT3 expression. To clarify whether TBM provides protection via SIRT3, we knockdown SIRT3 using siRNA before TBM treatment. Then, the cytoprotective effects of TBM were largely abolished by siSIRT3. This suggests that SIRT3 plays an essential role in TBM's endothelial protective effects and TBM might be a potential drug candidate to treat sepsis-induced endothelial dysfunction.

Introduction

Sepsis is life-threatening organ dysfunction caused by a deregulated host response to infection [1]. This new definition highlights the central role of organ dysfunction in the pathogenesis of sepsis. The occurrence of organ dysfunction is related to endothelial dysfunction [2, 3]. Cells which are located in the innermost layer of blood vessels are called endothelial cells, they form a semipermeable barrier and regulate vascular permeability, hemostasis, inflammation, and microcirculatory flow. In early sepsis, endothelial cell biomarkers of permeability and hemostasis are increased and vascular endothelial growth factor is reduced. And these changes are associated with increased mortality [4]. Therefore, developing novel therapeutic strategies for treating endothelial dysfunction in sepsis is of fundamental importance.

SIRT3 is a nicotinamide adenine dinucleotide (NAD^+)-dependent histone deacetylase, which is a member of the sirtuins family. Due to the diversity of protein targets, SIRT3 is a regulator of numerous cellular processes [5]. In recent years, SIRT3 was reported to function in endothelial metabolism, angiogenesis, and cardiovascular disease [6]. In sepsis, SIRT3 protects against acute kidney injury and cognitive dysfunction [7–9]. Although SIRT3 can protect against pericyte loss and microvascular dysfunction in the lung of septic mice [10], the underlying molecular mechanisms of SIRT3 in regulating endothelial dysfunction in sepsis have not been fully elucidated.

Tubeimoside I (TBM) is a triterpenoid saponin purified from tubeimu (the tuber of *Bolbostemma paniculatum* (Maxim.) Franquet) [11, 12]. In traditional Chinese medicine, tubeimu has been used to treat acute mastitis, snake bites, detoxication, inflammatory diseases, and tumors for

Supplementary information The online version contains supplementary material available at https://doi.org/10.1038/s41374-021-00580-y.

✉ Suxin Luo
luosuxin0204@163.com

✉ Jianghong Yan
yjhong1982@163.com

[1] Department of Cardiology, The First Affiliated Hospital of Chongqing Medical University, Chongqing, China

[2] Institute of Life Sciences, Chongqing Medical University, Chongqing, China

over 1000 years. In recent years, TBM was reported to possess good antineoplastic activity in many types of cancers [13–15]. TBM is also an effective anti-inflammatory drug [16–19]. However, the effect and the mechanisms of TBM in sepsis-induced endothelial dysfunction are unclear.

In this study, we detected that TBM could protect against sepsis-induced endothelial dysfunction by inhibiting oxidative stress and apoptosis both in vivo and in vitro. And its protective effects could be abolished by siSIRT3. These results demonstrated that TBM protected endothelium in sepsis via SIRT3 and TBM might be a new drug to treat sepsis-induced endothelial dysfunction.

Materials and methods

Materials

TBM (BP1415) was purchased from Chengdu Biopurify Technology Development Co. Ltd (www.biopurify.cn). Lipopolysaccharide (LPS) (L2880) was purchased from Sigma (St. Louis, MO, USA). Matrigel (356234) was purchased from BD (New York, NY, USA). Cell Counting Kit-8 (CCK8) (B34304) was purchased from Bimake (Houston, TX, USA). Reactive Oxygen Species (ROS) Assay Kit (S0033) was purchased from Beyotime (Shanghai, China). Primary antibodies against SOD2 (24127-1-AP), SIRT3 (10099-1-AP), GAPDH (60004-1-Ig), Bax (50599-2-Ig), Bcl-2 (12789-1-AP), and secondary antibodies (Goat anti-mouse, SA00001-1; Goat anti-rabbit, SA00001-2) were purchased from Proteintech Group (Chicago, IL, USA). Primary antibodies against cleaved caspase3 (#9664) and SIRT1 (#9475) were purchased from CST (Danvers, MA, USA). Primary antibodies against NADPH oxidase 2 (NOX2) (sc-130543) were purchased from Santa Cruz Biotechnology (Santa Cruz, CA, USA). Primary antibodies against Ac-SOD2 (ab137037) were purchased from Abcam (Cambridge Biomedical Campus, Cambridge, UK). All other reagents were obtained from common commercial sources.

Cell culture and treatment

Primary human umbilical vein endothelial cells (HUVECs) were isolated and cultivated as described previously [20]. Briefly, HUVECs were harvested by type I collagenase digestion at 37 °C and then cultured in M199 supplemented with 20% fetal bovine serum, 20 μg/ml endothelial cell growth supplement, 100 μg/ml heparin, 2 mM L-glutamine, and 1% penicillin and streptomycin. Six to ten passage cells were used for experiments. In experiments, HUVECs were digested with 0.25% trypsin and inoculated in six-well plates and grew to 80–90%. Then, cells were divided into four groups, those were Ctrl (control), TBM, LPS, and LPS + TBM. TBM (0–2 μM) was added to the TBM and LPS + TBM group, and 1 h later, LPS (10 μg/ml) was added to the LPS and LPS + TBM group. LPS treatment lasted for 12 or 24 h and cells were collected for detection. To confirm the function of SIRT3, siSIRT3 was transfected into LPS + TBM + siSIRT3 group cells before LPS treatment. siSIRT3 was designed using BLOCK-iT™ RNAi Designer (Thermo Scientific, Waltham, MA, USA) and synthesized by RiboBio (Guangzhou, China). Target sequences of siSIRT3 were GCAACCTCCAGCAGTACGA. Cells were transfected with siSIRT3 using Lipofectamine RNAiMax (Thermo Scientific, Waltham, MA, USA) according to the manufacturer's instructions. Twelve hours after siSIRT3 transfection, TBM was added. And LPS was added 1 h later after TBM was added. Note that cells should be washed with PBS and fresh media should be added to cells before adding drugs. And the volume of medium should be accurately measured with micropipette.

Animals

Wild-type male C57BL/6 mice were bought from the Laboratory Animal Center of Chongqing Medical University. Mice were raised in standard specific pathogen free room and were allowed free access to water and chow. Animal experiments were approved by the Animal Ethic Committee of Chongqing Medical University. And animal experiments were conducted according to the National and Institutional Guidelines for Animal Care and Use.

Cecal ligation and puncture (CLP)

Mice with weight of 25–30 g were subjected to CLP according to the protocol described by Rittirsch et al. [21]. Briefly, 20 mice were divided into four groups ($n = 5$/group), those were Ctrl, TBM, CLP, and CLP + TBM. PBS (Ctrl and CLP) or 4 mg/kg TBM (TBM and CLP + TBM) was given to mice by intraperitoneal injection 1 h before CLP. Then, mice were anesthetized by isoflurane inhalation. The cecum was exteriorized and ligated with 4-0 silk at 1/3 of the cecum. The distal cecum was punctured twice using a 21-gauge needle, and a small amount of feces was squeezed out to ensure patency of holes. The cecum was relocated to the cavum abdominis. The abdominal incision was closed in layers. To prevent dehydration, all mice were subcutaneously injected with sterile isotonic sodium chloride solution (5 ml per 100 g body weight). Ctrl mice underwent the same surgical procedures, except ligation and puncture.

Tissue preparation and vascular reactivity assay

At 12 h post CLP, mice were killed by cervical dislocation. Thoracic aortas and superior mesenteric arteries were

separated and placed in cold physiological salt solution (PSS) of the following composition: NaCl 119 mM, KCl 4.7 mM, $NaHCO_3$ 25 mM, $CaCl_2$ 2.5 mM, KH_2PO_4 1.2 mM, $MgSO_4$ 1.2 mM, and glucose 5.5 mM [22]. Adhering tissues were cleaned carefully to avoid destroying endothelial cells. Vessels were cut into 3-mm rings. Vascular reactivity assay was done using DMT620 system (Danish Myo Technology, Denmark). The arterial rings were mounted in chamber filled with warmed (37 °C), oxygenated (95% CO_2/5% O_2) PSS. Rings were equilibrated with 0.3 g resting tension for 60 min. Viability of the vessel was confirmed by two contractile responses to KCl (60 mM)-PSS. Cumulative dose–response curve was constructed to acetylcholine (Ach).

Western blotting

HUVECs or shredded mesenteric arteries were lysed on ice for 30 min using lysis buffer, and centrifuged at 12,000 × *g* for 15 min. Because many protein targets to be detected, we pooled mesenteric arteries of the same group of mice for protein extraction. Protein concentration of the supernatant was determined using the Bradford method and proper amount of protein was used for western blotting. Proteins were separated by sodium dodecyl sulfate polyacrylamide gel electrophoresis, transferred to polyvinylidene fluoride membranes, and probed with appropriate primary antibodies. Membrane-bound primary antibodies were detected with secondary antibodies which were conjugated with horseradish peroxidase. Finally, membranes were detected with chemiluminescence (Beyotime, Shanghai, China). Each protein target was detected four times. All four replicates were used for statistical analysis.

Morphological analysis

At 12 h post CLP, mice thoracic aortas were harvested and immersed in 4% paraformaldehyde at room temperature for at least 24 h. Samples were then embedded with paraffin, sectioned longitudinally into 5 μm thickness and deparaffinized with xylene. Finally, the slides were stained with HE and viewed by a Leica DM4B upright microscope (Leica, Heidelberg, Germany).

Tube formation assay

Matrigel was put into a 4 °C refrigerator to melt. Twenty-four-well plates and 1 ml tips were also put into the 4 °C refrigerator to cool. Matrigel (250 μl) were added into each well of a 24-well plate. The 24-well plate was incubated at 37 °C and 5% CO_2 for 30 min to solidify matrigel. HUVECs were digested and resuspended in culture media and cell concentration was 7×10^4/ml. HUVECs (3.5×10^4) were inoculated onto matrigel and cultivated at 37 °C and 5% CO_2 for 6 h. Tubes can be visualized and imaged using a phase contrast inverted microscope and number of meshes was analyzed using ImageJ (V.1.31).

For vessels, mice thoracic aortas were collected at 12 h post CLP and cut into 1-mm rings. Then, vessel rings were buried in the matrigel and proper volume of media was added. Vessel rings were cultivated at 37 °C and 5% CO_2 for about 1 week. Tubes can be visualized and imaged using a phase contrast inverted microscope and number of meshes was analyzed using ImageJ (V.1.31).

Cell viability assay

Cell viability was evaluated by CCK8 according to the manufacturer's instructions. Briefly, cells were digested with trypsin and seeded in 96-well plates at a density of 1×10^4 cells/well and cultured for 24 h. Then, cells were treated as described. At the end of treatment, culture media were removed and 100 μl of M199 together with 10 μl of the CCK8 solution were added to each well. Then, cells were incubated at 37 °C for 1–4 h. Finally, OD_{450} was detected using a microplate spectrophotometer (Thermo Scientific, Waltham, MA, USA). The effect of TBM on cell viability was expressed as the percentage cell viability compared with the Ctrl group which was set at 100%.

ROS detection

ROS was detected using ROS Assay Kit according to the manufacturer's instructions. Briefly, cells were seeded in six-well plates and cultured for 24 h. Then, cells were treated as described. At the end of treatment, culture media were removed and cells were washed with PBS. M199 containing 10 μM 2,7-dichlorodi-hydrofluorescein diacetate was added to each well. Then, cells were incubated at 37 °C for 20 min. Finally, cells were washed three times using PBS and imaged using a Leica DMI8 immunofluorescence microscope (Leica, Heidelberg, Germany). The excitation wavelength is 488 nm and the emission wavelength is 525 nm.

Statistical analysis

All data are presented as means ± standard deviation. All analyses were performed with GraphPad Prism 8.0 software. Comparisons between multiple groups were performed using one-way analysis of variance followed by Dunnett's post hoc test. $p < 0.05$ was taken as statistically significant.

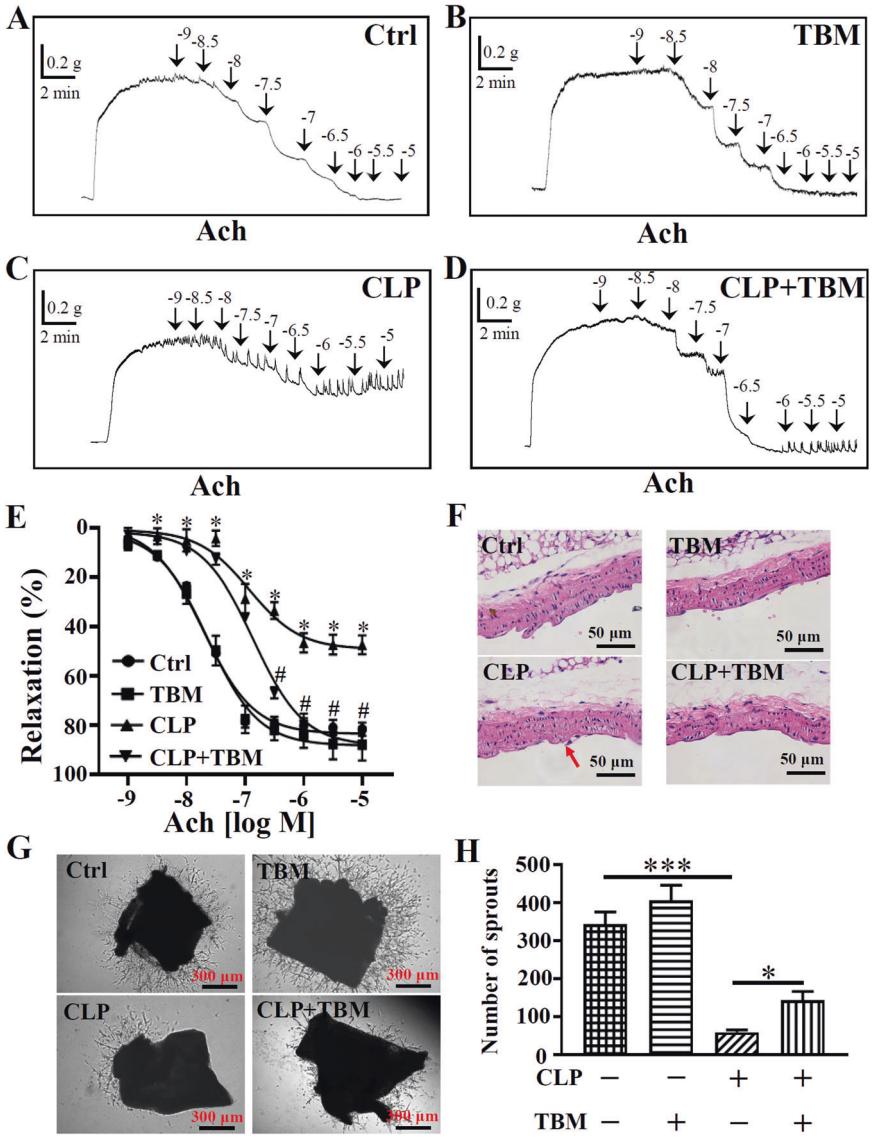

Fig. 1 TBM improved the structure and function of vascular endothelium in septic mice. Wild-type C57BL/6 mice ($n = 5$/group) subjected to CLP and mice were intraperitoneally injected with PBS (Ctrl and CLP group) or 4 mg/kg TBM (TBM and CLP + TBM group) 1 h before CLP. At 12 h post CLP, thoracic aortas were collected and examined using vascular reactivity assay, HE staining or capillary sprout assay. Representative raw tracings show concentration-dependent diastole to Ach (1 nM–10 μM) in the thoracic aorta taken from Ctrl (**A**), TBM (**B**), CLP (**C**), and CLP + TBM (**D**) mice. **E** The mean concentration–response curves elicited with cumulatively added Ach on the thoracic aorta obtained from different treatment groups. Differences among Ctrl, TBM, CLP, and CLP + TBM were analyzed using one-way analysis of variance (ANOVA) followed by Dunnett's post hoc test. Vertical bars represent standard deviation (SD). $^{*}p < 0.05$ compared with Ctrl; $^{\#}p < 0.05$ compared with CLP. **F** Representative HE staining images in each group. Red arrow indicates detached endothelial cells. Scar bar: 50 μm. **G** Representative images of vessel sprouts in each group. Scar bar: 300 μm. **H** Statistical analysis of sprouts in each group. Differences among Ctrl, TBM, CLP, and CLP + TBM were analyzed using one-way analysis of variance (ANOVA) followed by Dunnett's post hoc test. Data are expressed as means ± SD, $n = 4$. $^{*}p < 0.05$; $^{***}p < 0.001$.

Results

TBM improved the structure and function of vascular endothelium in septic mice

In sepsis, the structure and function of vascular endothelium are always destroyed. To assess whether TBM ameliorates vascular endothelial dysfunction in sepsis, we evaluated endothelial function using vascular reactivity assay at 12 h post CLP. As Fig. 1A–E shows, vascular reactivity to Ach (an indicator of endothelium-dependent diastolic function) was significantly decreased by CLP. But relaxation to Ach in TBM-treated mice was similar with that in Ctrl mice. Further, we detected the integrity of vascular endothelium using HE staining. CLP induced endothelial cells shed and TBM preserved the integrity of vascular endothelium

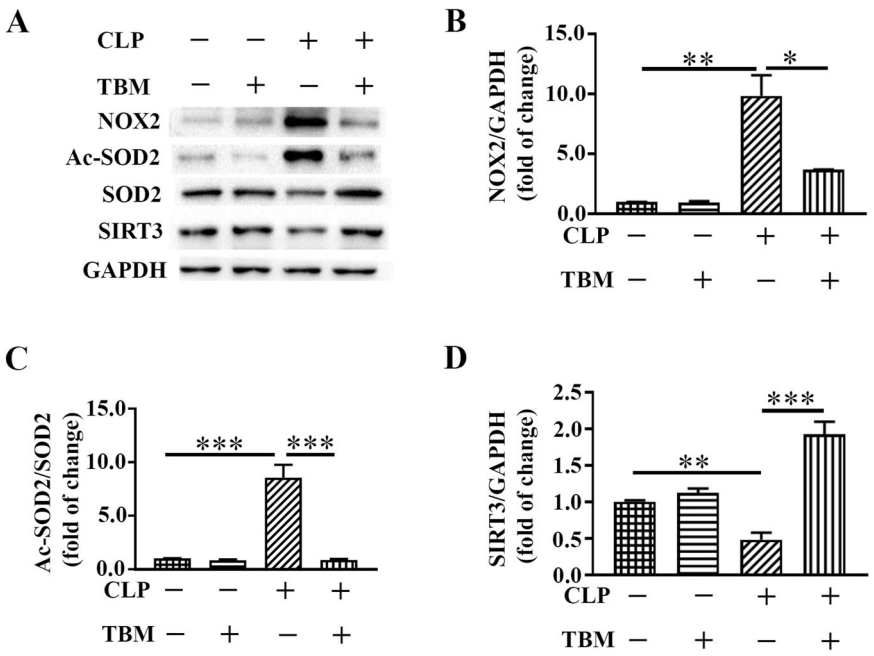

Fig. 2 TBM reduced oxidative stress of vessels in septic mice. Wild-type C57BL/6 mice ($n = 5$/group) subjected to CLP and mice were intraperitoneally injected with PBS (Ctrl and CLP group) or 4 mg/kg TBM (TBM and CLP + TBM group) 1 h before CLP. At 12 h post CLP, mesenteric arteries were collected and examined using western blotting. **A** Representative western blotting results of NOX2, Ac-SOD2, SOD2, and SIRT3. **B** Statistical analysis of the NOX2/GAPDH in each group. Differences among Ctrl, TBM, CLP, and CLP + TBM were analyzed using one-way analysis of variance (ANOVA) followed by Dunnett's post hoc test. Data are expressed as means ± SD, $n = 4$. $^{*}p < 0.05$; $^{**}p < 0.01$. **C** Statistical analysis of the Ac-SOD2/SOD2 in each group. Differences among Ctrl, TBM, CLP, and CLP + TBM were analyzed using one-way analysis of variance (ANOVA) followed by Dunnett's post hoc test. Data are expressed as means ± SD, $n = 4$. $^{***}p < 0.001$. **D** Statistical analysis of the SIRT3/GAPDH in each group. Differences among Ctrl, TBM, CLP, and CLP + TBM were analyzed using one-way analysis of variance (ANOVA) followed by Dunnett's post hoc test. Data are expressed as means ± SD, $n = 4$. $^{**}p < 0.01$; $^{***}p < 0.001$.

(Fig. 1F). Finally, we also detected the angiogenic capacity of endothelial cells using the aortic ring assay. As shown in Fig. 1G, H, TBM improved angiogenic capacity of septic mice vessels significantly. These results demonstrated that TBM could improve the structure and function of vascular endothelium in septic mice.

TBM reduced oxidative stress of vessels in septic mice

It was reported that sepsis-induced endothelial dysfunction was associated with oxidative stress. NOX2 is an essential superoxide producer, while superoxide dismutase (SOD2) is an important antioxidative molecule. Redox balance is influenced by activity of NOX2 and SOD2. And activity of SOD2 can be increased through deacetylation by SIRT3. To explore how TBM influenced oxidative stress in vivo, we detected NOX2, Ac-SOD2, SOD2, and SIRT3 in vessels by western blotting. NOX2 and Ac-SOD2/SOD2 were increased in CLP mice vessels, while TBM inhibited expression of NOX2 and the ratio of Ac-SOD2/SOD2 (Fig. 2A–C). Sepsis inhibited expression of SIRT3, while TBM restored expression of SIRT3 (Fig. 2A, D). These results implied that TBM effectively reduced oxidative stress of vessels in septic mice.

TBM inhibited apoptotic signaling pathway in vessels of septic mice

Apoptosis is a direct cause of endothelial dysfunction in sepsis. Thus, we detected whether TBM could relieve endothelial apoptosis in vivo using western blotting. As shown in Fig. 3, cleaved caspase3 and the ratio of Bax/Bcl-2 increased by CLP could be restored by TBM treatment. All these results demonstrated that TBM might exert protection by suppressing endothelial apoptosis in septic mice.

TBM improved cell viability and tube formation in LPS-treated HUVECs

To investigate TBM's effects on endothelium more directly, we isolated primary HUVECs and simulated CLP using LPS. As shown in Fig. 4, TBM could improve the cell viability and tube formation of HUVECs which were inhibited by LPS.

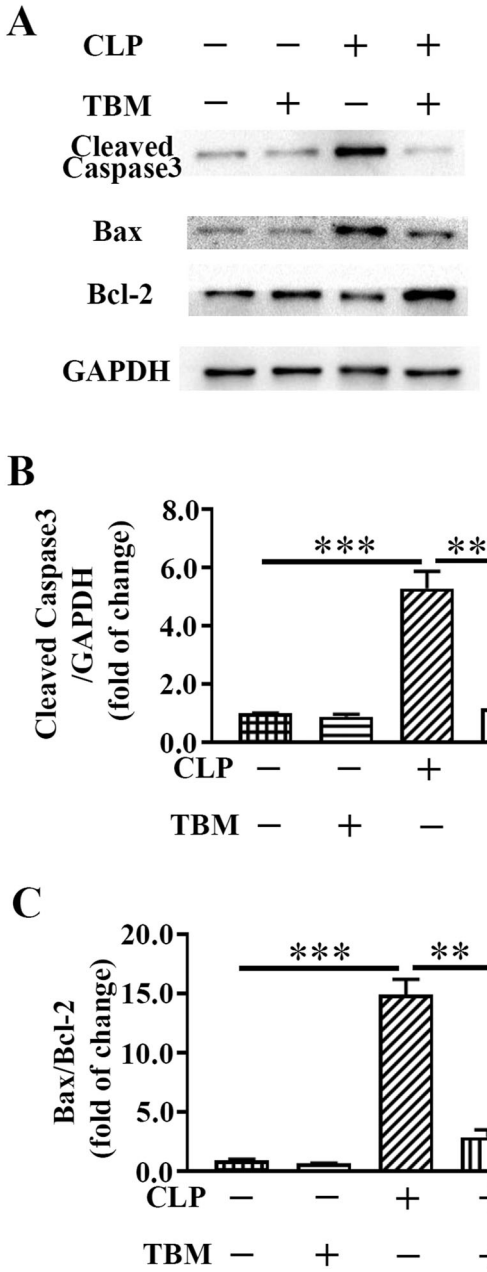

Fig. 3 TBM inhibited apoptotic signaling pathway in vessels of septic mice. Wild-type C57BL/6 mice ($n = 5$/group) subjected to CLP and mice were intraperitoneally injected with PBS (Ctrl and CLP group) or 4 mg/kg TBM (TBM and CLP + TBM group) 1 h before CLP. At 12 h post CLP, mesenteric arteries were collected and examined using western blotting. **A** Representative western blotting results of apoptotic proteins. **B** Statistical analysis of the cleaved caspase3/GAPDH in each group. Differences among Ctrl, TBM, CLP, and CLP + TBM were analyzed using one-way analysis of variance (ANOVA) followed by Dunnett's post hoc test. Data are expressed as means ± SD, $n = 4$. ***$p < 0.001$. **C** Statistical analysis of the Bax/Bcl-2 in each group. Differences among Ctrl, TBM, CLP, and CLP + TBM were analyzed using one-way analysis of variance (ANOVA) followed by Dunnett's post hoc test. Data are expressed as means ± SD, $n = 4$. **$p < 0.01$; ***$p < 0.001$.

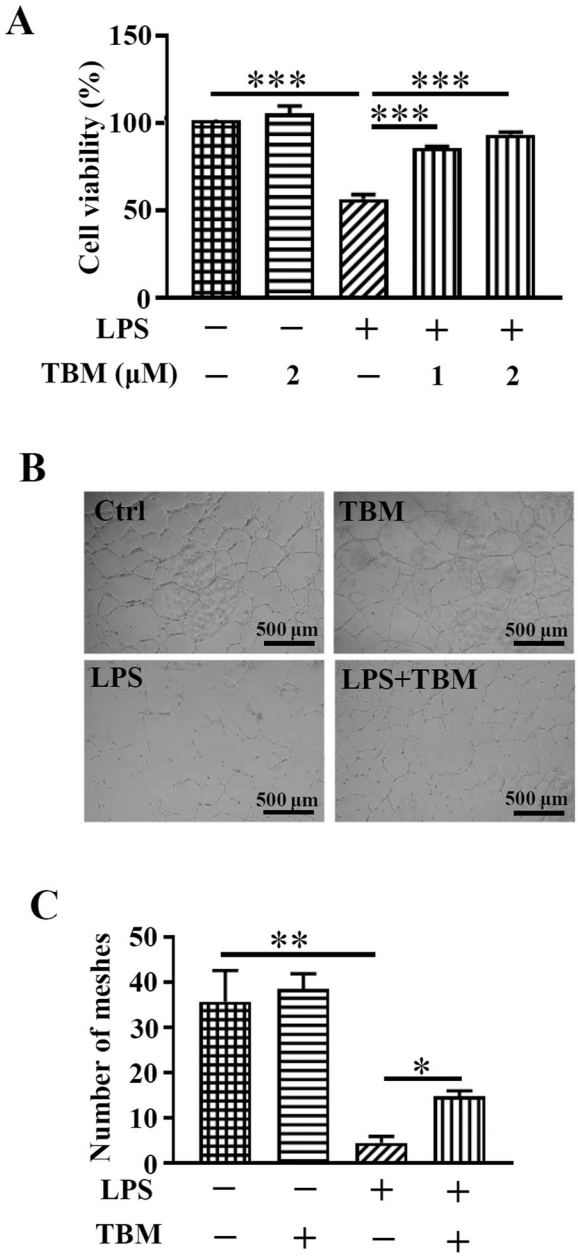

Fig. 4 TBM improved cell viability and tube formation in LPS-treated HUVECs. HUVECs were treated as described in materials and methods. TBM (0–2 μM) was added to the TBM and LPS + TBM group, and 1 h later, LPS (10 μg/ml) was added to the LPS and LPS + TBM group. After LPS treatment, cells were collected for detection using CCK8 (LPS treated for 24 h) or tube formation assay (LPS treated for 12 h). **A** Cell viability detected with CCK8. Differences among groups were analyzed using one-way analysis of variance (ANOVA) followed by Dunnett's post hoc test. Data are expressed as means ± SD, $n = 4$. ***$p < 0.001$. **B** Tube formation was detected using endothelial cell tube formation assay. Scar bar: 500 μm. **C** Statistical analysis of endothelial cell tube formation ability expressed as number of meshes. Differences among Ctrl, TBM, CLP, and CLP + TBM were analyzed using one-way analysis of variance (ANOVA) followed by Dunnett's post hoc test. Data are expressed as means ± SD, $n = 4$. *$p < 0.05$; **$p < 0.01$.

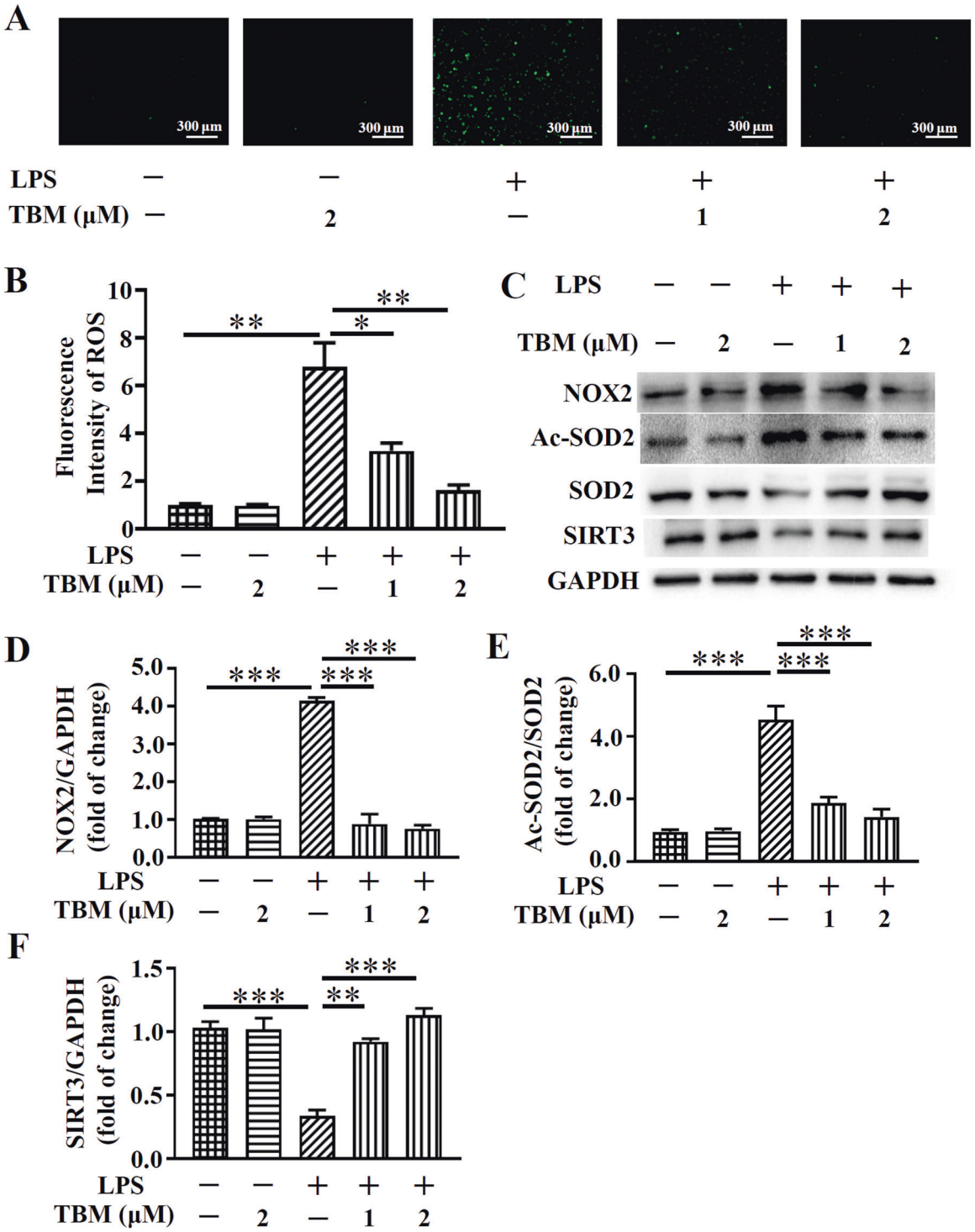

Fig. 5 TBM alleviated oxidative stress in LPS-treated HUVECs. HUVECs were treated as described in Fig. 4. Then, cells were examined using ROS assay kit or western blotting. **A** Representative results of ROS staining in each group. Scar bar: 300 μm. **B** Statistical analysis of ROS fluorescence intensity. The relative fluorescence intensity of ROS per field was determined using Image Pro Plus. Differences among groups were analyzed using one-way analysis of variance (ANOVA) followed by Dunnett's post hoc test. Data are expressed as means ± SD, $n = 4$. $^{*}p < 0.05$; $^{**}p < 0.01$. **C** Representative western blotting results of NOX2, Ac-SOD2, SOD2, and SIRT3. **D** Statistical analysis of the NOX2/GAPDH in each group. Differences among groups were analyzed using one-way analysis of variance (ANOVA) followed by Dunnett's post hoc test. Data are expressed as means ± SD, $n = 4$. $^{***}p < 0.001$. **E** Statistical analysis of the Ac-SOD2/ SOD2 in each group. Differences among groups were analyzed using one-way analysis of variance (ANOVA) followed by Dunnett's post hoc test. Data are expressed as means ± SD, $n = 4$. $^{***}p < 0.001$. **F** Statistical analysis of the SIRT3/GAPDH in each group. Differences among groups were analyzed using one-way analysis of variance (ANOVA) followed by Dunnett's post hoc test. Data are expressed as means ± SD, $n = 4$. $^{**}p < 0.01$; $^{***}p < 0.001$.

TBM alleviated oxidative stress and apoptosis in LPS-treated HUVECs

To illuminate the underlying mechanism, we investigated TBM's effects on oxidative stress and apoptosis in LPS-treated HUVECs. As shown in Fig. 5A, B, intracellular ROS enhanced by LPS was significantly inhibited by TBM. LPS increased expression of NOX2 and the ratio of Ac-SOD2/SOD2. While TBM could reverse these alterations (Fig. 5C–E). In addition, TBM could restore the expression of SIRT3 which was decreased in LPS-treated HUVECs (Fig. 5C, F).

Besides, we also determined the effects of TBM on apoptosis in LPS-treated HUVECs. We detected expression of key apoptotic proteins using western blotting. LPS induced a prominent apoptotic effect in HUVECs; TBM could resist apoptosis in a dose-dependent manner. The antiapoptotic effect of TBM was supported by decreased levels of cleaved caspase3 and Bax/Bcl-2 (Fig. 6)

SIRT3 plays an essential role in the cytoprotective effects of TBM in LPS-treated HUVECs

To examine SIRT3's function in the protective roles of TBM in LPS-treated HUVECs, we knockdown expression of SIRT3 using siRNA. First, we designed and synthesized a siSIRT3, and confirmed its efficiency and specificity using western blotting. As shown in Fig. S1, siSIRT3 could knockdown SIRT3 efficiently and specifically. Then, SIRT3's function in cell viability, antioxidative, and anti-apoptotic effects of TBM were examined. As Fig. 7A shown, siSIRT3 reversed the promotional effects of TBM on cell viability significantly. In addition, the inhibitive effects of TBM on NOX2 expression and the Ac-SOD2/SOD2 ratio were abolished by siSIRT3 (Fig. 7B–D). The antiapoptotic effect of TBM also largely abolished by siSIRT3. As shown in Fig. 7F–H, siSIRT3 increased cleaved caspase3 and Bax/Bcl-2 significantly. These results indicated that TBM might protect against sepsis-induced endothelial dysfunction through the SIRT3 signaling pathway.

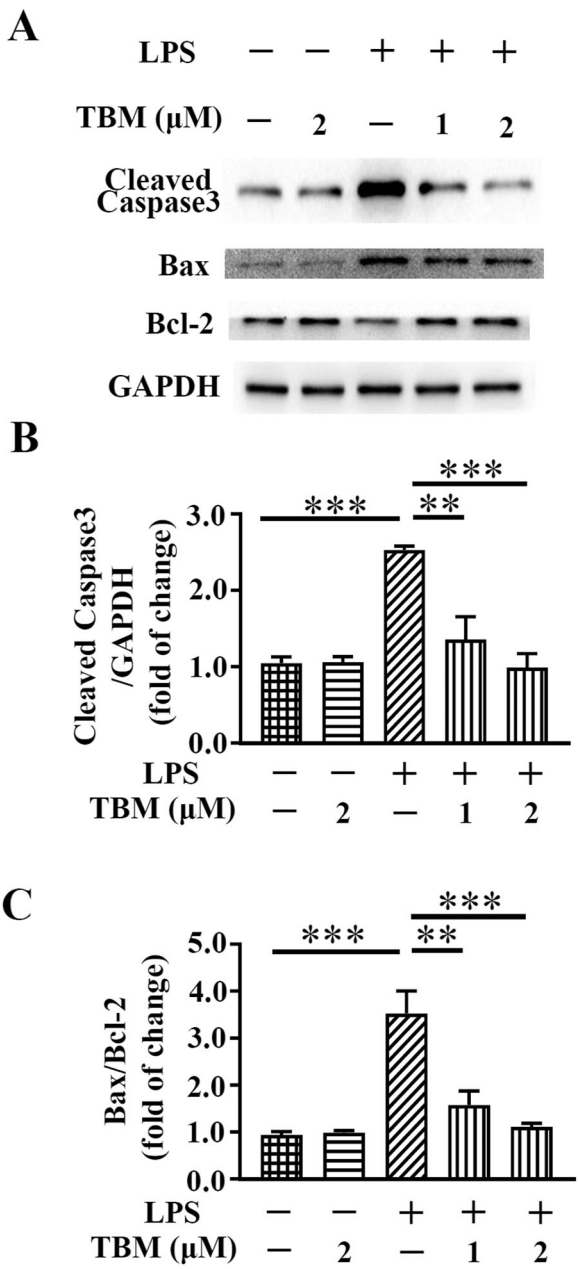

Fig. 6 TBM inhibited apoptotic signaling pathway in LPS-treated HUVECs. HUVECs were treated as described in Fig. 4. Then, cells were examined using western blotting. **A** Representative western blotting results of apoptotic proteins. **B** Statistical analysis of the cleaved caspase3/GAPDH in each group. Differences among groups were analyzed using one-way analysis of variance (ANOVA) followed by Dunnett's post hoc test. Data are expressed as means ± SD, $n = 4$. $^{**}p < 0.01$; $^{***}p < 0.001$. **C** Statistical analysis of the Bax/Bcl-2 in each group. Differences among groups were analyzed using one-way analysis of variance (ANOVA) followed by Dunnett's post hoc test. Data are expressed as means ± SD, $n = 4$. $^{**}p < 0.01$; $^{***}p < 0.001$.

Discussion

In this study, we examined the effects of TBM on endothelial function of septic mice. In vivo, TBM improved the integrity of endothelium, endothelium-dependent diastolic function, and angiogenic ability of vessels in septic mice. In vitro, TBM improved cell viability and tube formation of LPS-treated HUVECs. Also, our results demonstrated that TBM could inhibit oxidative stress and apoptosis caused by CLP or LPS. To unveil how TBM could inhibit oxidative stress and apoptosis, we knockdown expression of SIRT3 using siSIRT3. We found that TBM's protective effects on LPS-treated endothelial cells were abolished by siSIRT3. According to our results, TBM might protect against endothelial dysfunction via SIRT3.

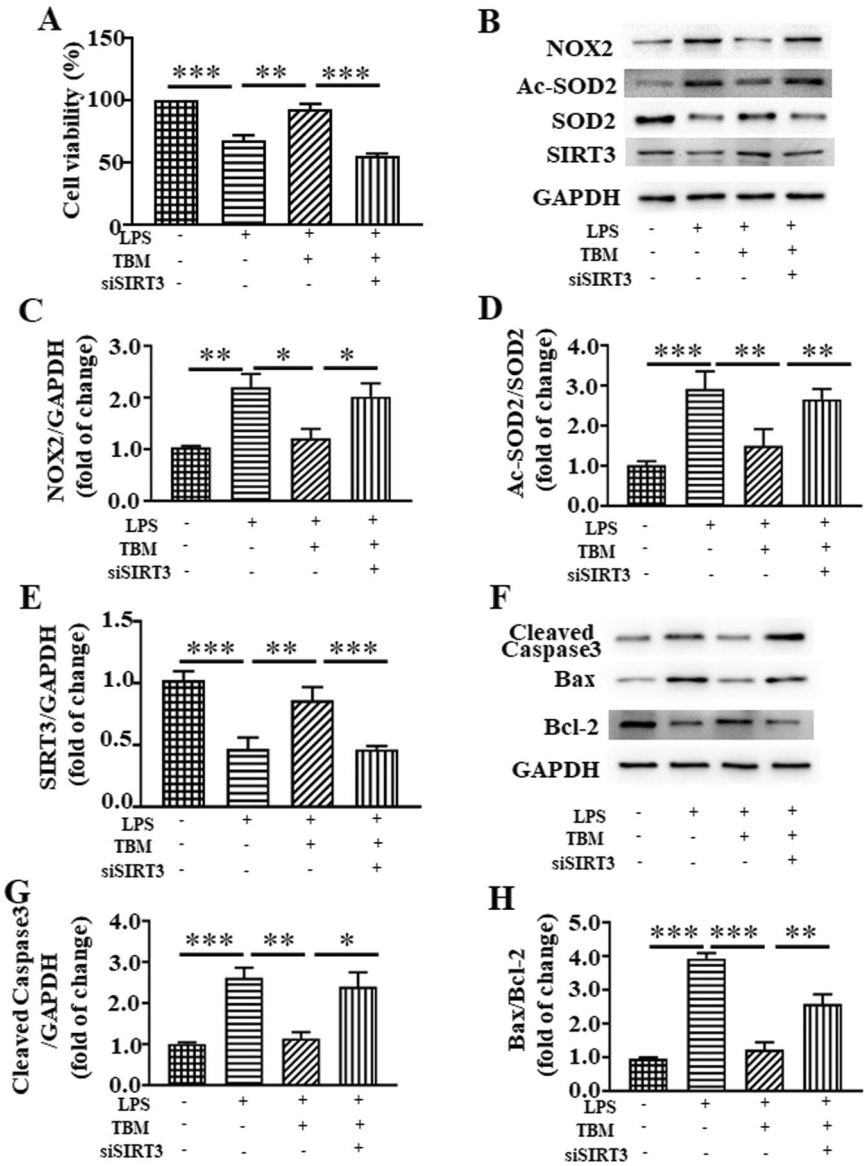

Fig. 7 Pretreatment of siSIRT3 abolished the cytoprotective effects of TBM in LPS-treated HUVECs. HUVECs were treated as described in Fig. 4. To confirm the function of SIRT3, siSIRT3 was transfected into the LPS + TBM + siSIRT3 group cells before LPS treatment. After LPS treatment, cells were collected for detection using CCK8 (LPS treated for 24 h) or western blotting (LPS treated for 12 h). **A** Cell viability detected with CCK8. Differences among groups were analyzed using one-way analysis of variance (ANOVA) followed by Dunnett's post hoc test. Data are expressed as means ± SD, $n = 4$. $^{**}p < 0.01$; $^{***}p < 0.001$. **B** Representative western blotting results of NOX2, Ac-SOD2, SOD2, and SIRT3. **C** Statistical analysis of the NOX2/GAPDH in each group. Differences among groups were analyzed using one-way analysis of variance (ANOVA) followed by Dunnett's post hoc test. Data are expressed as means ± SD, $n = 4$. $^{*}p < 0.05$; $^{**}p < 0.01$. **D** Statistical analysis of the Ac-SOD2/ SOD2 in each group. Differences among groups were analyzed using one-way analysis of variance (ANOVA) followed by Dunnett's post hoc test. Data are expressed as means ± SD, $n = 4$. $^{**}p < 0.01$; $^{***}p < 0.001$. **E** Statistical analysis of the SIRT3/GAPDH in each group. Differences among groups were analyzed using one-way analysis of variance (ANOVA) followed by Dunnett's post hoc test. Data are expressed as means ± SD, $n = 4$. $^{**}p < 0.01$; $^{***}p < 0.001$. **F** Representative western blotting results of apoptotic proteins. **G** Statistical analysis of the cleaved caspase3/GAPDH in each group. Differences among groups were analyzed using one-way analysis of variance (ANOVA) followed by Dunnett's post hoc test. Data are expressed as means ± SD, $n = 4$. $^{*}p < 0.05$; $^{**}p < 0.01$; $^{***}p < 0.001$. **H** Statistical analysis of the Bax/ Bcl-2 in each group. Differences among groups were analyzed using one-way analysis of variance (ANOVA) followed by Dunnett's post hoc test. Data are expressed as means ± SD, $n = 4$. $^{**}p < 0.01$; $^{***}p < 0.001$.

Sirtuins family contains seven members (SIRT1–7) [23]. Among these sirtuins, SIRT1 has been reported to play protective roles in a variety of organ injuries in sepsis, such as lung injury, kidney injury, liver injury, and heart injury [24–27]. But there is no study on SIRT1's effect on sepsis-induced endothelial dysfunction. We examined expression

of SIRT1 in septic vessels and LPS-treated HUVECs, and found that expression of SIRT1 was inhibited by CLP or LPS (Fig. S2). Although SIRT1 might play a role in sepsis-induced endothelial dysfunction, TBM treatment could not reverse reduced expression of SIRT1. This result demonstrated that TBM functioned via SIRT3 specifically.

Apart from TBM, several other drugs have been reported to protect against sepsis-induced endothelial dysfunction via SIRT3, such as polydatin, resveratrol, honokiol, and melatonin [7, 28–30]. Although all above drugs could induce the expression of SIRT3, their mechanisms are different. Polydatin, resveratrol, honokiol, and melatonin induced expression of SIRT3 through SIRT1–peroxisome proliferator activated receptor γ coactivator-1α signaling pathway. In our study, we did not observe inducible effect of TBM on expression of SIRT1. It would be meaningful to figure out how TBM induced expression of SIRT3. We analyzed the structure of TBM and found that it contained a structure (red box marked part in Fig. S3A) similar with estrogen (Fig. S3B). It was reported that transcription factor estrogen related receptors (EERs) could bind the SIRT3 promoter directly and regulate SIRT3 expression [31, 32]. We speculate that TBM induces expression of SIRT3 through EERs. We will test this hypothesis in future.

In sepsis, amounts of inflammatory factors are produced and they induced a great quantity of ROS [33, 34]. ROS damages the vascular endothelium of the whole body and ultimately leads to organs dysfunction [2, 33]. People have tried to treat sepsis by reducing ROS. At present, activated protein C is the only one drug approved by the Food and Drug Administration of the USA used to reduce ROS in sepsis. However, activated protein C is no longer used in the clinical treatment of sepsis due to its strong side effects and poor efficacy [35, 36]. In this study, our results demonstrated that TBM could alleviate sepsis-induced endothelial dysfunction. Previously, we have reported that TBM could improve survival of mice in sepsis [19]. All these results indicate that TBM is a promising new therapeutic agent against sepsis-induced endothelial dysfunction.

Our study has two limitations to be addressed. First, SIRT3 contains two isoforms, a long form (~44 kDa) and a short form (~28 kDa). The short form SIRT3 primarily resides in mitochondria and is more likely to exhibit deacetylase activity [37]. So, we examined the short form isoform of SIRT3 in this study. However, discrepancy of the two SIRT3 isoforms was demonstrated in a cardiac hypertrophy model [38]. Further studies need to be done concerning these two isoforms. Second, although we showed that TBM worked through SIRT3, we did not figure out the mechanism by which TBM increased SIRT3 in sepsis. We will study this in future.

In conclusion, the present data show for the first time that intraperitoneal injection of TBM alleviates sepsis-induced endothelial dysfunction. Our data suggest that TBM protects against sepsis-induced endothelial dysfunction by reducing oxidative stress and apoptosis via SIRT3. TBM is a promising new therapeutic agent against sepsis-induced endothelial dysfunction.

Funding This work was supported by the National Natural Science Foundation of China (31400999, 81400355, and 81770479), the Scientific and Technological Research Program of Chongqing Municipal Education Commission (KJQN201800417), and Basic Science and Frontier Technology Research Project of Chongqing Science and Technology Commission (cstc2020jcyj-msxmX1091 and cstc2017jcyjAX0330).

Author contributions XY performed the experiments and prepared the figures. XL conducted the CLP model. ML and CL helped in the animal studies. LH and XL helped in the detection of related indicators. BH and JS provided help for data analysis. SL and JY designed and supervised the study. JY analyzed data, prepared the figures, and wrote the manuscript. All authors reviewed and revised the final version of this manuscript and approved its submission.

Compliance with ethical standards

Conflict of interest The authors declare no competing interests.

Publisher's note Springer Nature remains neutral with regard to jurisdictional claims in published maps and institutional affiliations.

References

1. Singer M, Deutschman CS, Seymour CW, Shankar-Hari M, Annane D, Bauer M, et al. The third international consensus definitions for sepsis and septic shock (Sepsis-3). JAMA. 2016; 315:801–10.
2. Joffre J, Hellman J, Ince C, Ait-Oufella H. Endothelial responses in sepsis. Am J Resp Crit Care. 2020;202:361–70.
3. De Backer D, Cortes DO, Donadello K, Vincent JL. Pathophysiology of microcirculatory dysfunction and the pathogenesis of septic shock. Virulence. 2014;5:73–9.
4. Hou PC, Filbin MR, Wang H, Ngo L, Huang DT, Aird WC, et al. Endothelial permeability and hemostasis in septic shock: results from the ProCESS Trial. Chest. 2017;152:22–31.
5. Wu J, Zeng Z, Zhang W, Deng Z, Wan Y, Zhang Y, et al. Emerging role of SIRT3 in mitochondrial dysfunction and cardiovascular diseases. Free Radic Res. 2019;53:139–49.
6. He X, Zeng H, Chen JX. Emerging role of SIRT3 in endothelial metabolism, angiogenesis, and cardiovascular disease. J Cell Physiol. 2019;234:2252–65.
7. Xu S, Gao Y, Zhang Q, Wei S, Chen Z, Dai X, et al. SIRT1/3 activation by resveratrol attenuates acute kidney injury in a septic rat model. Oxidative Med Cell Longev. 2016;2016:7296092.
8. Sun F, Si Y, Bao H, Xu Y, Pan X, Zeng L, et al. Regulation of sirtuin 3-mediated deacetylation of cyclophilin D attenuated cognitive dysfunction induced by sepsis-associated encephalopathy in mice. Cell Mol Neurobiol. 2017;37:1457–64.
9. Zhao WY, Zhang L, Sui MX, Zhu YH, Zeng L. Protective effects of sirtuin 3 in a murine model of sepsis-induced acute kidney injury. Sci Rep. 2016;6:33201.
10. Zeng H, He X, Tuo QH, Liao DF, Zhang GQ, Chen JX. LPS causes pericyte loss and microvascular dysfunction via disruption of Sirt3/angiopoietins/Tie-2 and HIF-2α/Notch3 pathways. Sci Rep. 2016;6:20931.

11. Liu WY, Zhang WD, Chen HS, Gu ZB, Li TZ, Chen WS. New triterpenoid saponins from bulbs of *Bolbostemma paniculatum*. Planta Med. 2004;70:458–64.
12. Yu LJ, Ma RD, Wang YQ, Nishino H, Takayasu J, He WZ, et al. Potent anti-tumorigenic effect of tubeimoside 1 isolated from the bulb of *Bolbostemma paniculatum* (Maxim) Franquet. Int J Cancer. 1992;50:635–8.
13. Islam MS, Wang C, Zheng J, Paudyal N, Zhu Y, Sun H. The potential role of tubeimosides in cancer prevention and treatment. Eur J Med Chem. 2019;162:109–21.
14. Cao J, Zhao E, Zhu Q, Ji J, Wei Z, Xu B, et al. Tubeimoside-1 Inhibits glioblastoma growth, migration, and invasion via inducing ubiquitylation of MET. Cells. 2019;8:774.
15. Yan J, Dou X, Zhou J, Xiong Y, Mo L, Li L, et al. Tubeimoside-I sensitizes colorectal cancer cells to chemotherapy by inducing ROS-mediated impaired autophagolysosomes accumulation. J Exp Clin Cancer Res. 2019;38:353.
16. Bao Y, Li H, Li Q-Y, Li Y, Li F, Zhang C-F, et al. Therapeutic effects of Smilax glabra and *Bolbostemma paniculatum* on rheumatoid arthritis using a rat paw edema model. Biomed Pharmacother. 2018;108:309–15.
17. He D, Bingxu H, Shoupeng F, Yuhang L, Xin R, Yandan L, et al. Tubeimoside I protects dopaminergic neurons against inflammation-mediated damage in lipopolysaccharide (LPS)-evoked model of Parkinson's disease in rats. Int J Mol Sci. 2018;19:2242.
18. Zhang JB, Zhang L, Li SQ, Hou AH, Dai LL. Tubeimoside I attenuates inflammation and oxidative damage in a mice model of PM2.5-induced pulmonary injury. Exp Ther Med. 2017;15:1602–7.
19. Luo M, Luo S, Cheng Z, Yang X, Lv D, Li X, et al. Tubeimoside I improves survival of mice in sepsis by inhibiting inducible nitric oxide synthase expression. Biomed Pharmacother. 2020;126:110083.
20. Jianghong Y, Qianyi W, Suxin L, Yong X. A detailed protocol to cultivate and identify human umbilical endothelial cells. J Xinjiang Med Univ. 2016;39:555–9.
21. Rittirsch D, Huber-Lang MS, Flierl MA, Ward PA. Immunodesign of experimental sepsis by cecal ligation and puncture. Nat Protoc. 2009;4:31–6.
22. Yadav VR, Nayeem MA, Tilley SL, Mustafa SJ. Angiotensin II stimulation alters vasomotor response to adenosine in mouse mesenteric artery: role for A1 and A2B adenosine receptors. Brit J Pharmacol. 2015;172:4959–69.
23. Chang HC, Guarente L. SIRT1 and other sirtuins in metabolism. Trends Endocrinol Metab. 2014;25:138–45.
24. Chen S, Ding R, Hu Z, Yin X, Xiao F, Zhang W, et al. MicroRNA-34a inhibition alleviates lung injury in cecal ligation and puncture induced septic mice. Front Immunol. 2020;11:1829.
25. Su H, Ma Z, Guo A, Wu H, Yang X. Salvianolic acid B protects against sepsis-induced liver injury via activation of SIRT1/PGC-1α signaling. Exp Ther Med. 2020;20:2675–83.
26. Liu P, Shi D. Calcitonin gene-related peptide attenuates LPS-induced acute kidney injury by regulating Sirt1. Med Sci Monit. 2020;26:e923900.
27. Smith LM, Yoza BK, Hoth JJ, McCall CE, Vachharajani V. SIRT1 mediates septic cardiomyopathy in a murine model of polymicrobial sepsis. Shock. 2020;54:96–101.
28. Wu J, Deng Z, Sun M, Zhang W, Yang Y, Zeng Z, et al. Polydatin protects against lipopolysaccharide-induced endothelial barrier disruption via SIRT3 activation. Lab Investig. 2020;100:643–56.
29. Chen L, Li W, Qi D, Lu L, Zhang Z, Wang D. Honokiol protects pulmonary microvascular endothelial barrier against lipopolysaccharide-induced ARDS partially via the Sirt3/AMPK signaling axis. Life Sci. 2018;210:86–95.
30. Zhai M, Li B, Duan W, Jing L, Zhang B, Zhang M, et al. Melatonin ameliorates myocardial ischemia reperfusion injury through SIRT3-dependent regulation of oxidative stress and apoptosis. J Pineal Res. 2017;63:e12419.
31. Giralt A, Hondares E, Villena JA, Ribas F, Díaz-Delfín J, Giralt M, et al. Peroxisome proliferator-activated receptor-gamma coactivator-1alpha controls transcription of the Sirt3 gene, an essential component of the thermogenic brown adipocyte phenotype. J Biol Chem. 2011;286:16958–66.
32. Kong X, Wang R, Xue Y, Liu X, Zhang H, Chen Y, et al. Sirtuin 3, a new target of PGC-1alpha, plays an important role in the suppression of ROS and mitochondrial biogenesis. PLoS ONE. 2010;5:e11707.
33. Gu M, Mei XL, Zhao YN. Sepsis and Cerebral Dysfunction: BBB damage, neuroinflammation, oxidative stress, apoptosis and autophagy as key mediators and the potential therapeutic approaches. Neurotox Res. 2020. https://doi.org/10.1007/s12640-020-00270-5.
34. Prauchner CA. Oxidative stress in sepsis: pathophysiological implications justifying antioxidant co-therapy. Burns. 2017;43:471–85.
35. Riewald M, Ruf W. Protease-activated receptor-1 signaling by activated protein C in cytokine-perturbed endothelial cells is distinct from thrombin signaling. J Biol Chem. 2005;280:19808–14.
36. Ward PA, Bosmann M. A historical perspective on sepsis. Am J Pathol. 2012;181:2–7.
37. Garrity J, Gardner JG, Hawse W, Wolberger C, Escalante-Semerena JC. N-lysine propionylation controls the activity of propionyl-CoA synthetase. J Biol Chem. 2007;282:30239–45.
38. Sundaresan NR, Gupta M, Kim G, Rajamohan SB, Isbatan A, Gupta MP. Sirt3 blocks the cardiac hypertrophic response by augmenting Foxo3a-dependent antioxidant defense mechanisms in mice. J Clin Investig. 2009;119:2758–71.